

See discussions, stats, and author profiles for this publication at: <https://www.researchgate.net/publication/263946150>

Excellent Catalytic Effects of Graphene Nanofibers on Hydrogen Release of Sodium alanate

ARTICLE *in* THE JOURNAL OF PHYSICAL CHEMISTRY C · MAY 2012

Impact Factor: 4.77 · DOI: 10.1021/jp300934h

CITATIONS

14

READS

31

10 AUTHORS, INCLUDING:



[M. Sterlin Leo Hudson](#)

National Institute of Standards and Technology

21 PUBLICATIONS 232 CITATIONS

[SEE PROFILE](#)



[Ralph H. Scheicher](#)

Uppsala University

188 PUBLICATIONS 1,241 CITATIONS

[SEE PROFILE](#)



[Biswarup Pathak](#)

Indian Institute of Technology Indore

60 PUBLICATIONS 589 CITATIONS

[SEE PROFILE](#)



[C. Moyses Araujo](#)

Uppsala University

82 PUBLICATIONS 1,233 CITATIONS

[SEE PROFILE](#)

Excellent Catalytic Effects of Graphene Nanofibers on Hydrogen Release of Sodium alanate

Zhao Qian,^{*,†,‡} M. Sterlin Leo Hudson,[§] Himanshu Raghubanshi,[§] Ralph H. Scheicher,[‡] Biswarup Pathak,[‡] C. Moysés Araújo,[‡] Andreas Blomqvist,^{‡,⊥} Börje Johansson,^{†,‡} O. N. Srivastava,^{*,§} and Rajeev Ahuja^{*,†,‡}

[†]Department of Materials Science and Engineering, Applied Materials Physics, KTH Royal Institute of Technology, SE-100 44 Stockholm, Sweden

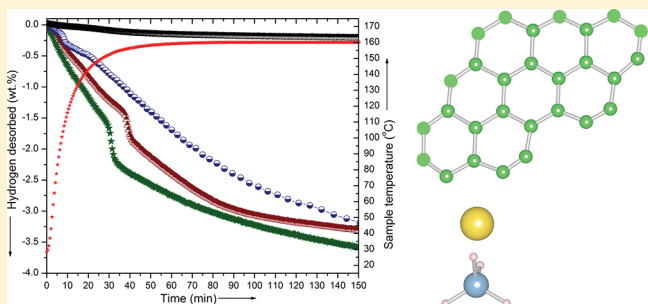
[‡]Condensed Matter Theory Group, Department of Physics and Astronomy, Ångström Laboratory, Uppsala University, SE-751 20 Uppsala, Sweden

[§]Nanoscience and Technology Unit, Department of Physics, Banaras Hindu University, Varanasi 221010, India

[⊥]Sandvik Tooling R&D, Lerkrogsvägen 13, Stockholm, Sweden

Supporting Information

ABSTRACT: One of the most technically challenging barriers to the widespread commercialization of hydrogen-fueled devices and vehicles remains hydrogen storage. More environmentally friendly and effective nonmetal catalysts are required to improve hydrogen sorption. In this paper, through a combination of experiment and theory, we evaluate and explore the catalytic effects of layered graphene nanofibers toward hydrogen release of light metal hydrides such as sodium alanate. Graphene nanofibers, especially the helical kind, are found to considerably improve hydrogen release from NaAlH₄, which is of significance for the further enhancement of this practical material for environmentally friendly and effective hydrogen storage applications. Using density functional theory, we find that carbon sheet edges, regardless of whether they are of zigzag or armchair type, can weaken Al–H bonds in sodium alanate, which is believed to be due to a combination of NaAlH₄ destabilization and dissociation product stabilization. The helical form of graphene nanofibers, with larger surface area and curved configuration, appears to benefit the functionalization of carbon sheet edges. We believe that our combined experimental and theoretical study will stimulate more explorations of other microporous or mesoporous nanomaterials with an abundance of exposed carbon edges in the application of practical complex light metal hydride systems.



INTRODUCTION

Hydrogen storage remains one among several technically challenging barriers to the widespread commercialization of hydrogen-fueled devices.¹ While hydrogen has the highest energy content per unit weight of any fuel, it has a low energy content per unit volume, which poses a challenge for storage.² Much research has been carried out to find the most suitable material(s) for hydrogen storage systems to meet the technical goals of both reaching a storage density of 1.8 kWh/kg (5.5% hydrogen by weight) and 1.3 kWh/L (40 g H₂/L)³ and maintaining favorable thermodynamics as well as fast kinetics.⁴ Sodium alanate (NaAlH₄) has been proposed to be one of the most practical hydrogen storage materials which can meet the required DOE 2015 target. However, proper catalysts are required to improve the hydrogen sorption and lower the desorption temperature of NaAlH₄.⁵

Since the pioneering work of catalyzing NaAlH₄ with titanium by Bogdanovic and Schwickardi,⁶ many transition metal catalysts^{7–11} have been extensively studied to promote

the hydrogen storage properties of NaAlH₄. Although showing good catalyzing effects, some metal-based catalysts often suffer from multiple competitive disadvantages including high cost, low selectivity, poor durability, and detrimental environmental effects caused by metal catalyst residues.¹² Therefore, it is essential to develop some inexpensive, nonmetal catalysts of high performance,¹³ which is of significance to realize the sustainable chain of hydrogen economy considering both environmental compatibility and low costs. Carbon nanomaterials are becoming increasingly recognized for their use in promoting hydrogen storage.¹⁴ The fiber form of carbon possesses the potential for large-scale production because of the mass and green wood sources on earth. In this context, we have explored both experimentally and theoretically the catalytic effects on NaAlH₄ exerted by graphene nanofibers which are

Received: January 29, 2012

Revised: April 17, 2012

Published: April 26, 2012

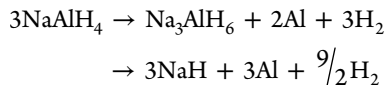
composed of layered graphene stacks. State-of-the-art ab initio theoretical tools are used to understand the mechanism behind the catalytic effects. It is proposed to promote more investigations of other microporous or mesoporous nanomaterials with an abundance of exposed carbon edges in practical complex light metal hydride systems applications.

MATERIALS AND METHODS

Helical graphene nanofiber (HGNF) and planar graphene nanofiber (PGNF) were synthesized through the dissociation of hydrocarbon gas (acetylene/ethylene) over Ni nanoparticles catalyst at 650 °C under a flow of He and H₂ gas, both with an optimized flow rate of 1500 sccm. The growth of HGNF has been achieved by employing faceted Ni nanoparticles, whereas spherical Ni nanoparticles produce PGNF. The synthesis-acquired metal impurities on GNFs were purified by acid treatment using concentrated HCl. The GNFs were thermally annealed at 400 °C under inert atmosphere to remove the oxygen complexes and defects to increase the graphitic order of GNFs. The FTIR spectra of GNFs thus obtained does not reveal any signature of C—H, C—O, or C=O. SWCNT (OD: ~1 nm) was supplied by M K Impex Corp. Canada. Admixing was performed by mechanically mixing NaAlH₄ (Aldrich, 93%) with carbon nanovariants together with two steel balls of 12.5 mm diameter each and one ball of 4 mm diameter using a locally fabricated chrome-nickel stainless steel mixer for 15 min. All operations on the samples were performed under dry argon atmosphere in a glovebox. The dehydrogenation behaviors of hydrogen storage systems were monitored using a computerized pressure composition temperature (PCT) isotherm measurement system supplied by Advanced Materials Corporation (Pittsburgh, PA). The sample weighing 0.5 g was loaded in the sample chamber for dehydrogenation measurements. Temperature-programmed desorptions (TPD) of the samples were carried out using the same PCT measurement system under dynamic heating conditions by programming the furnace at a constant heating rate of 1, 2, 5, and 10 °C/min.

RESULTS AND DISCUSSION

Hydrogen desorption from NaAlH₄ takes place mainly through the following reactions:



An effective catalyst makes these reactions feasible under moderate temperature and pressure. In the present study, we have synthesized two forms of layered graphene nanofibers and explored their catalytic effects on NaAlH₄. Figure 1a–d brings out the microstructures of the HGNF, the PGNF, and the HGNF-admixed NaAlH₄ as well as the selected area electron diffraction (SAED) pattern (obtained using 10 μm selected area aperture) of 2 wt% HGNF-admixed NaAlH₄. The inset in Figure 1a,b shows the corresponding SAED patterns of HGNF and PGNF, respectively. The SAED pattern of 2 wt% HGNF-admixed NaAlH₄ corresponding to Figure 1c is shown in Figure 1d. As depicted in the insets, the SAED pattern of HGNF contains four (002) arc spots, whereas for PGNF only two (002) arc spots were observed, which suggests different configurations of GNFs. It has been noticed that after admixing with NaAlH₄, the HGNFs are broken into small pieces. However, from the SAED pattern of 2 wt% HGNF-admixed

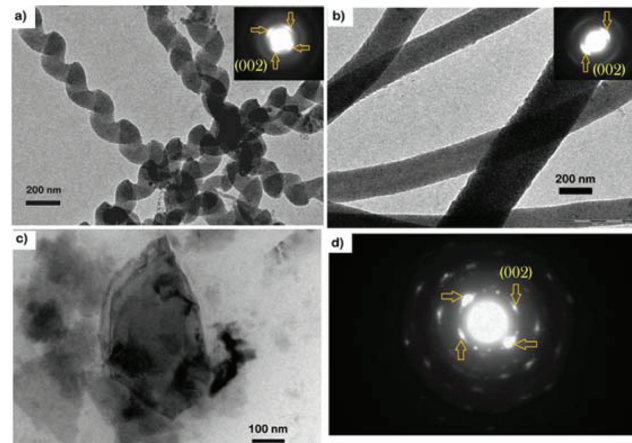


Figure 1. Transmission electron micrograph of (a) HGNF used in experiment, (b) PGNF used in experiment, (c) HGNF-admixed NaAlH₄, and (d) SAED pattern of 2 wt% HGNF-admixed NaAlH₄.

NaAlH₄ (Figure 1d), it becomes clear that the configuration of GNF is not completely disturbed upon admixing with NaAlH₄.^{15,16}

Figure 2 shows the TPD curve of NaAlH₄ admixed with 2 wt% carbon nanovariants. In the desorption experiment, single-

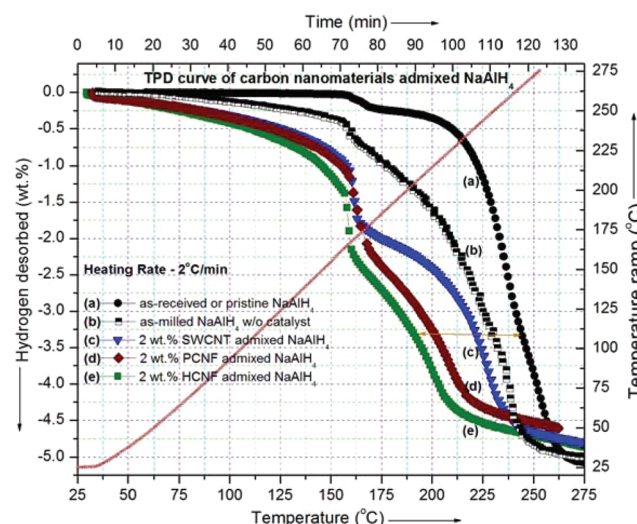


Figure 2. TPD curves of NaAlH₄ admixed with 2 wt% carbon nanovariants as specified in the figure (the red dotted line represents the sample heating profile).

walled carbon nanotubes (SWCNT) with outer diameter ~1 nm (supplied by MK Impex Canada) were used for comparison. In addition, a control experiment was carried out in which NaAlH₄ was subjected to the same ball-milling procedure as that used for mixing with the carbonaceous nanomaterials. As evident in Figure 2, when admixed with 2 wt% graphene nanofibers, the dehydrogenation behavior of NaAlH₄ is improved significantly. At the heating rate of 2 °C/min, the temperature corresponding to the total dehydrogenation of 3.5 wt% H₂ has been lowered from 246 °C (pristine NaAlH₄) to 182 °C (2 wt% HGNF-admixed sodium alanate). For 2 wt% PGNF and 2 wt% SWCNT-admixed NaAlH₄, it is 193 °C and 214 °C, respectively. Ball milling the pristine NaAlH₄ alone will also lead to some improvement in

the hydrogen desorption properties. However, the effect is clearly seen to be not as strong as for those cases when SWCNT or GNF was added.

Representative plots from our desorption kinetics study are shown in Figure 3. The desorption kinetics of 2 wt.% HGNF-

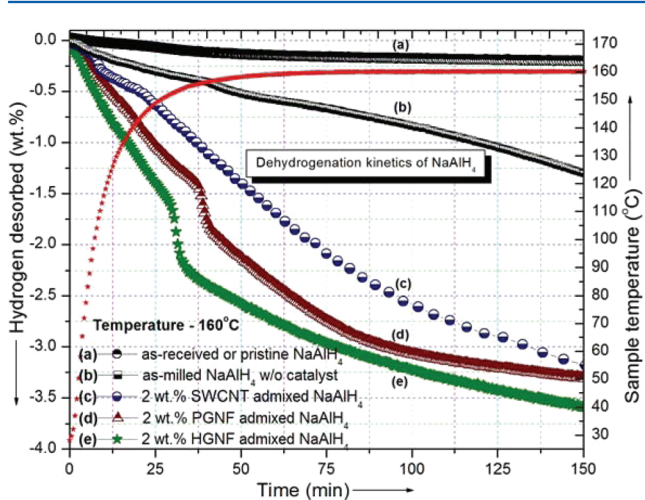


Figure 3. Desorption kinetic curves of 2 wt.% carbon nanovariant admixed NaAlH_4 .

admixed NaAlH_4 was carried out at 160 °C. Comparative studies on the hydrogen desorption from 2 wt.% PGNF and from 2 wt.% SWCNT-admixed NaAlH_4 were also carried out. It has been observed that the hydrogen desorption from 2 wt.% GNF-admixed NaAlH_4 is superior to that of 2 wt.% SWCNT-admixed NaAlH_4 . Especially for the helical one, the tested catalytic effect is significantly better.

The experimental results thus clearly demonstrate that nanostructured carbon has a strong catalytic effect on the hydrogen desorption from NaAlH_4 . It is also clear, however, that GNFs work better than SWCNTs as catalysts. The basic constituents of those two types of carbon nanostructures is graphene, rolled up into a tube for SWCNTs and stacked on top of each other in the GNFs (with some variations in the long-range stacking arrangement between HGNFs and PGNFs). The main difference between the two types appears to be the exposed graphene edges in the case of GNFs. Thus, we set ourselves the task to answer the question whether exposed graphene edges in GNFs can indeed explain the catalytic action upon hydrogen desorption from NaAlH_4 . In order to study the fundamental mechanism behind the catalytic effects of layered graphene nanofibers, we modeled the interaction of sodium alanate with various edge sites of one single-layer graphene patch from first-principles theory. Both zigzag edge and armchair edge are considered for our study to understand their catalytic activities toward hydrogen release from NaAlH_4 . In our experiment, the nanofibers used could have a diameter of 150 nm (huge for atomistic simulation); still, at some point, steps will occur where the edge structure changes from zigzag to armchair, and we can simulate these steps. Also, we restrain those atoms that would be bonded to other carbon atoms within the layer from geometry relaxations. The molecular approach is used here as we successfully utilized previously, to mimic the properties of the hydride solid.^{17,18} The calculated 1.6–1.7 Å lengths of Al–H bonds in the pristine NaAlH_4 cluster and the hydrogen removal energy from the pristine NaAlH_4 cluster (3.8 eV) agree very well with the corresponding values in bulk crystalline NaAlH_4 .^{19,20} In our previous study, the curvature effect of carbon nanostructures has been investigated, while in the present investigation, we show the significance of catalytic effects of zigzag and armchair

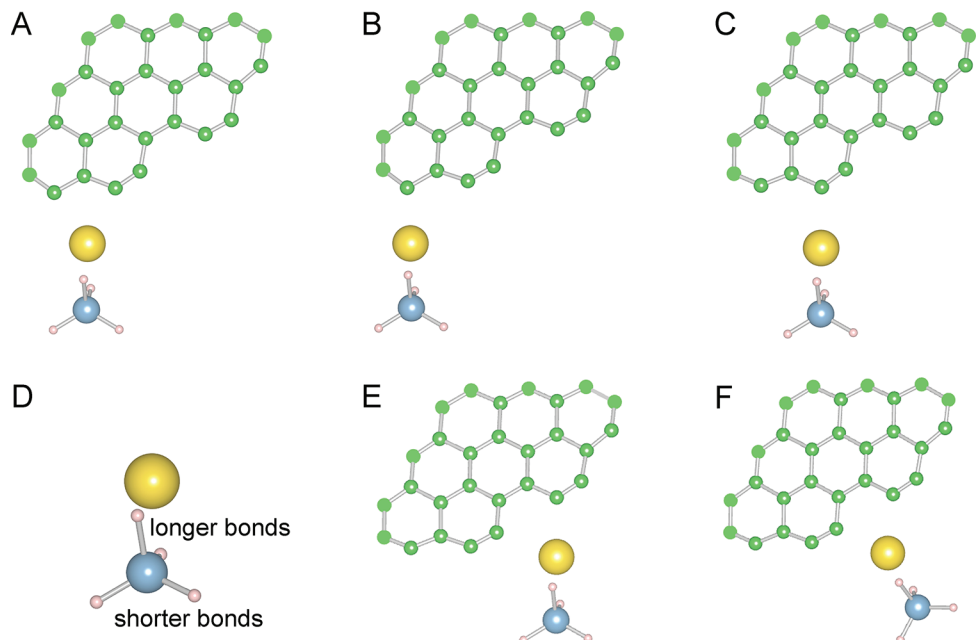


Figure 4. Equilibrium configurations of NaAlH_4 positions with the Na atom facing various sites of carbon edges (zigzag or armchair edge) and of the isolated NaAlH_4 cluster: A–C, sites at zigzag edge; D, isolated one for comparison; E and F, sites at armchair edge (Note: these designations are also used in the following Figures 5, 6, and 7). Na atoms are shown in the color of yellow, Al in blue, H in pink, and C in green. The color of “filled” light green in all carbon sheets above means the corresponding carbon atoms are fixed in modeling to simulate the restraining effect that those would experience that are bonded to other carbon atoms within the same graphene layer.

carbon edges. We carefully considered all kinds of carbon edge sites that could possibly interact with NaAlH_4 . The simulations are based on density functional theory^{21,22} using the projector-augmented wave (PAW) method²³ and generalized gradient approximation (GGA).²⁴ The Vienna Ab Initio Simulation Package (VASP) code^{25–27} was used in our calculations. The cutoff for planewave expansion is 470 eV. Visualization for structural analysis was carried out through Visualization for Electronic and Structural Analysis (VESTA).²⁸

Figure 4 shows the equilibrium configurations of the NaAlH_4 clusters facing various sites at zigzag or armchair edges of the graphene patch as well as that of the pristine NaAlH_4 cluster (without any carbon edge, designated as D in Figure 4 for comparison). In Figure 4, A–C correspond to cases where NaAlH_4 has been placed near various sites at the zigzag edge; E and F are the cases for the armchair edge. In all cases, the Al–H bonds of the NaAlH_4 cluster are carefully divided into two longer Al–H bonds and two shorter Al–H bonds. In the following study, we systematically investigate the effects of graphene edges on the Al–H bonds and determine if they lead to a weakening of the bonds, which we interpret as improving the associated hydrogen release kinetics from NaAlH_4 .

The value of hydrogen removal energy can reflect the strength of hydrogen–host bonds. In this study, the hydrogen removal energies of NaAlH_4 in all cases were thoroughly calculated. We considered hydrogen removal from the longer Al–H bond and from the shorter Al–H bond, respectively, in all cases of Figure 4A–F. Figure 5 shows the results. Compared

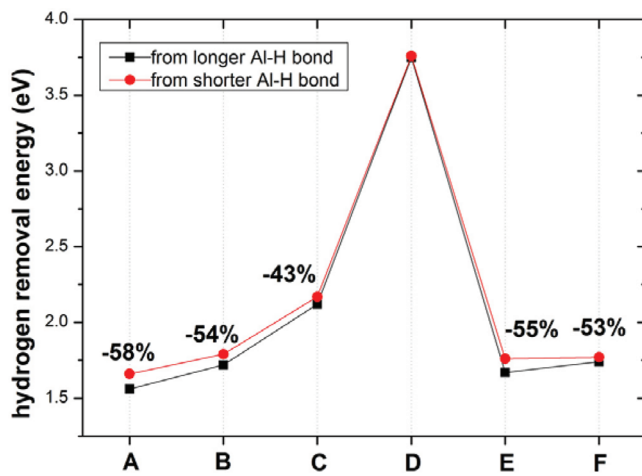


Figure 5. Effects of various carbon edge sites on the hydrogen removal energies of NaAlH_4 . A–F correspond to the various cases shown in Figure 4.

with the value of the case D (i.e., the isolated or pristine NaAlH_4), the hydrogen removal energies of NaAlH_4 when placed near a carbon edge (independent of whether it is a zigzag or armchair edge) are found to be greatly decreased. The hydrogen removal energy from the longer Al–H bond and that from the shorter Al–H bond shows similar trends. In the case of zigzag edge sites, i.e., A, B and C, the decrease of hydrogen removal energy can be as large as 58%; that is, the hydrogen removal energy can be lowered to 1.56 eV at site A, which is much lower than the 3.8 eV of the pristine NaAlH_4 . Sites B and C also show considerable effects on the hydrogen removal energy, with decreases by 54% and 43%, respectively. As for the armchair edge sites, similarly, E and F also exhibit good effects,

leading to evident decreases of hydrogen removal energy, respectively. Therefore, carbon edges, both of the zigzag edge or the armchair edge type, are capable of weakening the Al–H bonds and thus decrease the hydrogen removal energy of sodium alanate considerably. This is of great significance for improving the kinetics of this material for potential hydrogen storage. Also note that these decreased hydrogen removal energies are lower than those of NaAlH_4 mixed with fullerene C_{60} or carbon nanotubes (with hydrogen removal energies of around 3 eV).¹⁷ This might help to explain our experimental observation that graphene nanofibers (GNFs) possess better catalytic activity on the hydrogen release of NaAlH_4 than that of SWCNTs. This result is also consistent with the superiority of GNFs over SWCNTs in terms of lowering the activation energy for the hydrogen desorption from NaAlH_4 as estimated experimentally in Figures S1 and S2 of the Supporting Information.

As explained above, all Al–H bonds (both longer and shorter Al–H bonds) are actually weakened by the carbon edges. So what is the underlying reason for this bond weakening? To further explore the origin, we first checked the actual changes in the bond lengths. Different than expected, the upper panel of Figure 6 shows that only the shorter Al–H bonds display an elongating trend (i.e., bond lengths become larger when NaAlH_4 is placed near carbon edges) that could correspond with the trend of decreasing bond strengths shown in Figure 5, while the longer Al–H bonds contract (i.e., become shorter)

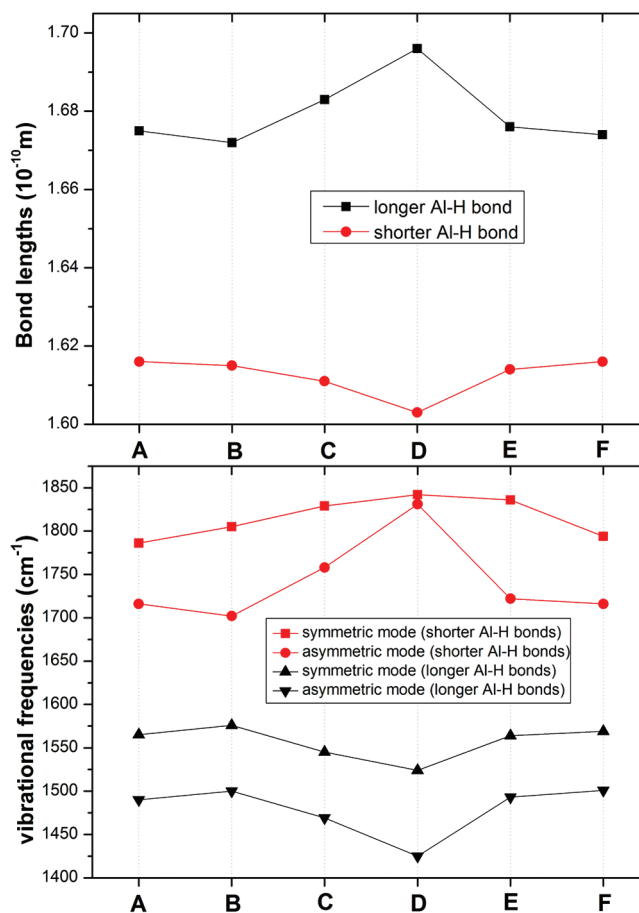


Figure 6. (Upper panel) Changes of Al–H bonds lengths in various models. (Lower panel) Vibrational frequency investigations of all Al–H bonds in various models.

when NaAlH_4 is near the carbon edges. This behavior cannot explain the weakening of both types of Al–H bonds (i.e., longer bonds and shorter bonds). The lower panel of Figure 6 gives the tested information of vibrational frequencies and focuses on Al–H vibration modes. Similarly, only the trends of shorter Al–H bonds (red curves, including both symmetric and asymmetric modes) are as one would expect; for the longer Al–H bonds, the frequencies increase when the carbon edges affect the NaAlH_4 cluster, indicating a stiffening of the bonds rather than the expected weakening. In fact, if carefully compared, the trends of bond lengths correspond very well with those of the vibrational frequencies in Figure 6, although they failed to give the origin for the weakening of all Al–H bonds.

To further explore and better understand the origin of the bonds weakening, we performed an electronic charge analysis^{29–31} to investigate the charge transfer circumstances before and after the hydrogen removal from NaAlH_4 , respectively, when in near-contact with the carbon edges. Before the hydrogen removal, i.e., for the reactant sodium alanate, the charge transfer circumstance to various carbon edge sites is shown in the upper panel of Figure 7. Compared with the case D of pure or pristine NaAlH_4 , the charge transfer occurs from Na to any of the carbon edge sites but with significant differences between the various sites. For the zigzag

edge sites A and B, the highest charge transfer is found, followed in magnitude by the armchair sites E and F, while finally the charge transfer is lowest for the zigzag site C. Interestingly, this trend of charge transfer corresponds with those of the hydrogen removal energies shown in Figure 5. As previously explained,¹⁷ the stability of NaAlH_4 originates with the charge transfer from Na to the AlH_4^- moiety, resulting in an ionic bond between Na^+ and AlH_4^- and stabilizing the covalent bonds between Al and the four H atoms. Here, the carbon edges “grab” some charge and thus would affect the normal charge donation of Na to AlH_4^- , which leads to the destabilization of reactant NaAlH_4 . Generally, the zigzag edge can attract more charge from NaAlH_4 compared with the armchair edge, which means that the zigzag edge can destabilize sodium alanate more.

The lower panel of Figure 7 gives the charge analysis of the AlH_3 moiety after one hydrogen removal from the reactant NaAlH_4 . Both the hydrogen removal from the longer Al–H bond and the removal from the shorter Al–H bond are considered. Actually, the two display similar trends. Compared with the case D of pristine NaAlH_4 , the charge state of the AlH_3 moiety becomes nearly zero in any case of those NaAlH_4 models with assistance from the carbon edges. At both the zigzag edge sites (A, B, C) and the armchair edge sites (E, F), after one hydrogen is removed from NaAlH_4 , the charges of Na transfer to the carbon edges instead of to the AlH_3 moiety, which makes the AlH_3 moiety nearly neutral. Our previous cluster investigation revealed that, among AlH_n clusters, AlH_3 without charge is the most stable one.¹⁷ Thus in this study, because of the existence of assisting carbon edges, the removal or dissociation product has evidently been stabilized. The graphene patch edges can play the role of both destabilizing the reactant NaAlH_4 and stabilizing the removal product, which is thought to be the reason for the evident decrease of hydrogen dissociation energies in Figure 5. In other words, the Al–H bond weakening is a combination of reactant destabilization and product stabilization.

As shown in Figure 5, the graphene patch edges can effectively decrease the hydrogen removal energy of NaAlH_4 (to less than 2 eV). GNFs consist of large amounts of graphene patch layers, which can supply a large quantity of exposed carbon sheet edges. Thus, GNFs could perform as very good nanocatalysts to improve hydrogen sorption of NaAlH_4 . Especially the helical form of GNFs, with surface areas larger than that of the planar GNF and thus more carbon edges, would be ideal for this catalytic role.

CONCLUSION

Through a combination of experiment and theory, the catalytic effects of graphene nanofibers on NaAlH_4 , one of the most explored and practical hydrogen storage materials, have been demonstrated and explained. Graphene nanofibers, especially in their helical form, can considerably improve the hydrogen release of NaAlH_4 . This is of significance for the further enhancement of this material for environmentally friendly hydrogen storage. Using density functional theory, we have investigated the underlying mechanism for the catalytic effectiveness of graphene nanofibers. The carbon sheet edges, both at their zigzag edge and at the armchair edge, lead to a weakening of the Al–H bonds in NaAlH_4 and, as a result, drastically decrease the hydrogen removal energy. This bond-weakening is shown to be due to a combination of NaAlH_4 destabilization and dissociation product stabilization. A side

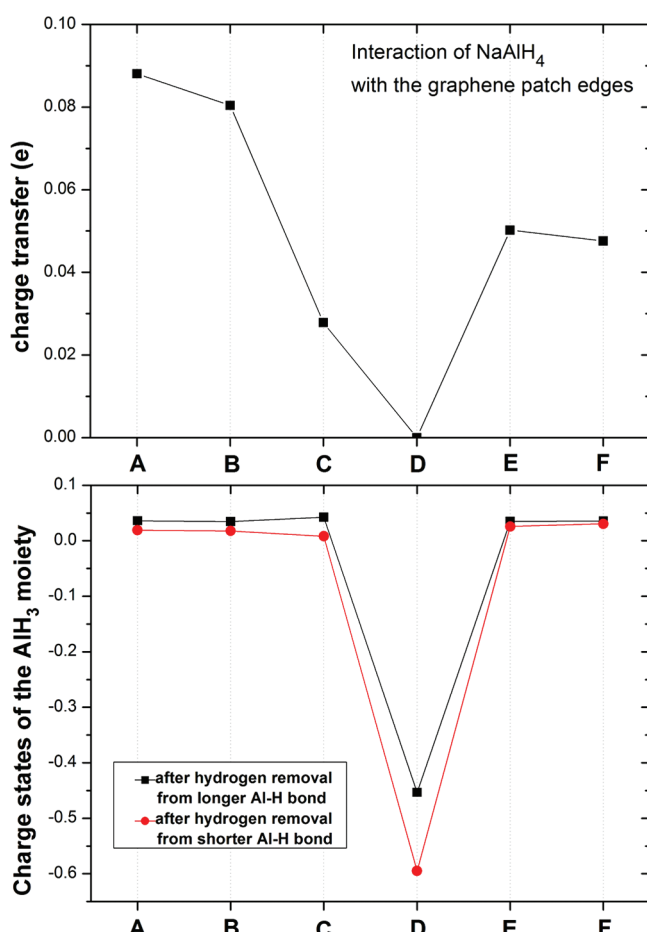


Figure 7. (Upper panel) Charge transfer from Na to various carbon edge sites before hydrogen removal from NaAlH_4 . (Lower panel) Charge states of the AlH_3 moiety in all cases after one hydrogen has been removed from NaAlH_4 .

finding is the intimate correlation between Al–H vibration modes and Al–H bond lengths. We propose that in the future other microporous or mesoporous nanomaterials with an abundance of exposed carbon edges should be tried as catalysts for the practical complex light metal hydride systems.

■ ASSOCIATED CONTENT

Supporting Information

TPD plots of carbon nanovariant-admixed NaAlH₄ at different heating rates and the estimated activation energies. This material is available free of charge via the Internet at <http://pubs.acs.org>.

■ AUTHOR INFORMATION

Corresponding Author

*E-mail: zhaoq@kth.se (Z.Q.), hepons@yahoo.com (O.N.S.), rajeev.ahuja@fysik.uu.se (R.A.).

Notes

The authors declare no competing financial interest.

■ ACKNOWLEDGMENTS

We thank Prof. P. Jena for fruitful discussions in Uppsala. Financial support is gratefully acknowledged from the Ministry of New and Renewable Energy, the University Grants Commission, Department of Science and Technology and the Council of Scientific and Industrial Research (India), FORMAS, Wenner-Gren Foundations, the Swedish Research Council (VR), the Swedish Foundation for International Cooperation in Research and Higher Education (STINT), and the China Scholarship Council. The Swedish National Infrastructure for Computing (SNIC), the Uppsala Multi-disciplinary Center for Advanced Computational Science (UPPMAX), and National Supercomputer Centre (NSC) provided computing time for this project.

■ REFERENCES

- (1) Weidenthaler, C.; Felderhoff, M. *Energy Environ. Sci.* **2011**, *4*, 2495–2502.
- (2) Schlapbach, L.; Züttel, A. *Nature* **2001**, *414*, 353–358.
- (3) Yang, J.; Sudik, A.; Wolverton, C.; Siegel, D. *J. Chem. Soc. Rev.* **2010**, *39*, 656–675.
- (4) Chen, P.; Zhu, M. *Mater. Today* **2008**, *11* (12), 36–43.
- (5) Gross, K. J.; Thomas, G. J.; Jenson, C. M. *J. Alloys Compd.* **2002**, *330*–*332*, 683–690.
- (6) Bogdanovic, B.; Schwickardi, M. *J. Alloys Compd.* **1997**, *253*–*254*, 1–9.
- (7) Bogdanovic, B.; Felderhoff, M.; Pommerin, A.; Schüth, F.; Spielkamp, N. *Adv. Mater.* **2006**, *18*, 1198–1201.
- (8) Zidan, R. A.; Takara, S.; Hee, A. G.; Jensen, C. M. *J. Alloys Compd.* **1999**, *285*, 119–122.
- (9) Sandrock, G.; Gross, K.; Thomas, G. *J. Alloys Compd.* **2002**, *339*, 299–308.
- (10) Anton, D. L. *J. Alloys Compd.* **2003**, *356*–*357*, 400–404.
- (11) Sakintuna, B.; Lamari-Darkrim, F.; Hirscher, M. *Int. J. Hydrogen Energy* **2007**, *32*, 1121–1140.
- (12) Yu, D.; Nagelli, E.; Du, F.; Dai, L. *J. Phys. Chem. Lett.* **2010**, *1*, 2165–2173.
- (13) Jeon, K. J.; Moon, H. R.; Ruminski, A. M.; Jiang, B.; Kisielowski, C.; Bardhan, R.; Urban, J. *J. Nature Mat.* **2011**, *10*, 286–290.
- (14) Teprovich, J. A.; Wellons, M. S.; Lascola, R.; Hwang, S. J.; Ward, P. A.; Compton, R. N.; Zidan, R. *Nano Lett.* **2012**, *12*, 582–589.
- (15) Jung, H. S.; Lee, S. Y.; Ahn, J. P.; Park, J. K. *Met. Mater. Int.* **2006**, *12*, 417–423.
- (16) Gulijk, C. V.; Lathouder, K. M. D.; Haswell, R. *Carbon* **2006**, *44*, 2950–2956.
- (17) Berseth, P. A.; Harter, A. G.; Zidan, R.; Blomqvist, A.; Araújo, C. M.; Scheicher, R. H.; Ahuja, R.; Jena, P. *Nano Lett.* **2009**, *9*, 1501–1505.
- (18) Scheicher, R. H.; Li, S.; Araújo, C. M.; Blomqvist, A.; Ahuja, R.; Jena, P. *Nanotechnology* **2011**, *22*, 335401.
- (19) Araújo, C. M.; Ahuja, R.; Osorio Guillén, J. M.; Jena, P. *Appl. Phys. Lett.* **2005**, *86*, 251913.
- (20) Araújo, C. M.; Li, S.; Ahuja, R.; Jena, P. *Phys. Rev. B* **2005**, *72*, 165101.
- (21) Hohenberg, P.; Kohn, W. *Phys. Rev.* **1964**, *136*, B864–B871.
- (22) Kohn, W.; Sham, L. *J. Phys. Rev.* **1965**, *140*, A1133–A1138.
- (23) Blöchl, P. E. *Phys. Rev. B* **1994**, *50*, 17953–17979.
- (24) Perdew, J. P.; Wang, Y. *Phys. Rev. B* **1986**, *33*, 8800–8802.
- (25) Kresse, G.; Hafner, J. *Phys. Rev. B* **1993**, *48*, 13115–13118.
- (26) Kresse, G.; Furthmüller, J. *Phys. Rev. B* **1996**, *54*, 11169–11186.
- (27) Kresse, G.; Furthmüller, J. *J. Comput. Mater. Sci.* **1996**, *6*, 15–50.
- (28) Momma, K.; Izumi, F. *J. Appl. Crystallogr.* **2008**, *41*, 653–658.
- (29) Tang, W.; Sanville, E.; Henkelman, G. *J. Phys.: Condens. Matter* **2009**, *21*, 084204.
- (30) Sanville, E.; Kenny, S. D.; Smith, R.; Henkelman, G. *J. Comput. Chem.* **2007**, *28*, 899–908.
- (31) Henkelman, G.; Arnaldsson, A.; Jónsson, H. *Comput. Mater. Sci.* **2006**, *36*, 354–360.